Sensors & Transducers Journal, Vol. 137, Issue 2, February 2012, pp. 47-58

www.sensorsportal.com

Sensors & Transducers

ISSN 1726-5479
© 2012 by IFSA
http://www.sensorsportal.com

Properties and Gas Sensing Mechanism Study of CTO Thin Films as Ethanol Sensor

[1] GANESH E. PATIL, [1] D. D. KAJALE, [2] V. B. GAIKWAD, [3] N. K. PAWAR, [1,*] G. H. JAIN

[1] Materials Research Lab., Arts, Commerce and Science College, Nandgaon 423 106 India
[2] Materials Research Lab., K.T.H.M. College, Nashik 422 005 India
[3] Dept. of Physics, K.A.A.N.M. Sonanwane Arts, Commerce & Science College, Satana 423301 India
[*] Tel.: +91 9423474476
E-mail: gotanjain@rediffmail.com (G.H. Jain)

Received: 8 November 2011 /Accepted: 14 February 2012 /Published: 28 February 2012

Abstract: Cr doped tin oxide (CTO) thin films were prepared by spray pyrolysis technique (SPT). The hollow microspheres with a high Cr incorporation (10 at. %) was found to posses excellent sensitivity, selectivity and rapid response to the presence of ethanol vapors at low temperature. X-ray diffraction, UV, scanning electron microscopy and energy dispersive X-ray analysis were carried out to investigate the gas sensing mechanism. The optical study showed that the films have a band gap of 3.54 eV. *Copyright © 2012 IFSA.*

Keywords: Cr doped tin oxide, Thin films, Spray pyrolysis, Sensing mechanism.

1. Introduction

Hydrocarbon gases, widely used as industrial and domestic fuels, have often proved to be hazardous because of explosions caused by leaks. It is therefore of vital importance to develop good sensors for hydrocarbon gases. Metal oxide gas sensors are the most commercialized type of gas sensors. Semiconductor metal oxides, such as tin oxide, zinc oxide, titanium oxide, zirconium oxide, indium oxide, etc have long been investigated as sensing materials [1-7]. Unfortunately, such problems as poor selectivity and long term stability have not been solved throughout. An improvement of these properties requires a better understanding of the sensing mechanisms. Recent developments and current status of semiconducting gas sensors have been reviewed by some authors [8-13]. In this area, tin oxide (SnO_2) sensor material has been widely applied as a basic material in gas sensors primarily

due to its high sensitivity and low cost [14]. In SnO_2 sensors, the gas sensing mechanism can be described in terms of an adsorption/desorption process of oxygen at the surface of a sensing element. Thus, for the complete description of sensor response, the interactions between the sensor element and the target gas should be clarified. The reaction mechanism of alcohol detection by tin oxide films was extensively investigated to understand the nature of alcohol gas detection. In particular, Ogawa et al. [15], Kohl [16] and Rao et al. [17] reported the interaction of ethanol vapor with a SnO_2 surface. However, generally recognized poor selectivity and low thermodynamic stability of SnO_2 at elevated temperatures have given rise to the search for new active materials. Additives, such as metal oxides, are known to improve the sensitivity and selectivity of SnO_2 sensors. The acidic Al_2O_3 and basic La_2O_3 additives are known to improve the sensitivity to CO and ethanol, respectively [18, 19]. There are no reports dealing with Cr doped tin oxide (CTO) ethanol sensors. Efforts have therefore been made to develop Cr doped tin oxide thin film gas sensors for the detection of ethanol vapors and for the improvement in its sensing performance of the thin films.

Spray pyrolysis technique (SPT) is useful alternative to the traditional methods for obtaining thin films. It is of particular interest because of its simplicity, low cost and minimal waste production. In this technique, a solution consisting of the ions of required compound is sprayed on a heated substrate and their pyrolysis results in deposition of the compound in thin film form. The chemical reactants are selected such that the products other than the desired compound are volatile at the temperature of deposition [20]. The aim of the present work is to develop the sensor with CTO thin films prepared by spray pyrolysis technique, which could be able to detect the ethanol vapors.

2. Experimental

A 0.01 M aqueous methanol solution of a mixture of chromium oxide (Sigma-Aldritch) and $SnCl_4.5H_2O$ (Sigma-Aldritch), Cr:Sn=1:9 mole ratio, was chosen as the precursor for the preparation of CTO thin films. The experimental arrangement for preparation of CTO thin film is shown Fig. 1. Air was employed as the carrier gas, and the substrate temperature was 350 ^oC. The glass substrates were ultrasonically pre-treated in acetone and ethanol, followed by ultrasonic cleaning in distilled water prior to deposition. The solution was sprayed continuously through a glass nozzle of 0.1 mm inner diameter onto glass substrate. The film deposition was performed by repeating two identical procedures, with a 10 min. break between them. A procedure involved two steps, each consisting of 10 s spraying, followed by 30 s pause. The deposition parameters like spray rate 5 ml/min. was adjusted using air as a carrier gas, nozzle to substrate distance (25 cm) were kept constant, and to and fro frequency of the nozzle (18 cycles min^{-1}) were kept constant at the optimized values indicated in brackets [21, 22].

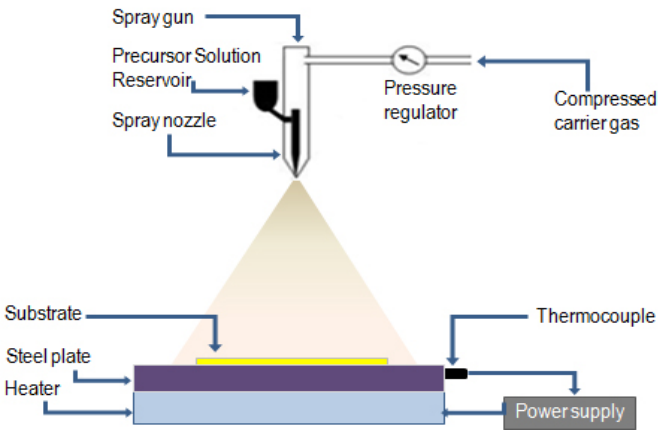

Fig. 1. Spray pyrolysis unit.

2.1. Formation of CTO Thin Film

The sprayed droplets undergo solvent evaporation, solute condensation and thermal decomposition, thereby resulting in the formation of thin films. 0.1 % of chromium dopant in the tin matrix was achieved using of Cr^{6+} containing oxide (CrO_3, 99.9 %). In solution, Cr^{6+} reduces to Cr^{3+}, following the equations:

$$CrO_3 + H_2O \rightarrow H_2CrO_4 \quad (1)$$

or

$$2CrO_3 + H_2O \rightarrow H_2Cr_2O_7 \quad (2)$$

The necessary water for hydrolysis was supplied from the solution itself, since the methanol solution contained 4 % water. The obtained acids are unstable and reduce to Cr^{3+}, in alcohol solution:

$$2H_2CrO_4 \rightarrow Cr_2O_3 + 3/2O_2 + 2H_2O \quad (3)$$

$$H_2Cr_2O_7 \rightarrow Cr_2O_3 + 3/2O_2 + H_2O \quad (4)$$

The pyrolytic reaction takes place on a heated substrate, leading to a nano-crystalline metal oxide. The usual expression for this reaction is:

$$SnCl_4.5H_2O \xrightarrow{350\ ^oC} SnO_2 + 4HCl + 3H_2O \quad (5)$$

For the Cr-doped films, it can be written:

$$(1-x)SnO_2 + x/2Cr_2O_3 \rightarrow Cr_xSn_{1-x}O_{2-\delta}\ , \quad (6)$$

where $Cr_xSn_{1-x}O_{2-\delta}$ is the chemical composition of the obtained films, with the atomic percentage of chromium: x=0.1 % .

As prepared SnO_2 thin film was annealed at 550 ^oC for 30 min. The phase and crystallinity of CTO thin films were recorded on X-ray diffractometer (Miniflex Model, Rigaku, Japan) using CuK_α radiation with a wavelength λ =1.5418 A^o at 2θ values between 20^o and 80^o. The average crystallite size (D) was estimated using the Scherrer equation [23] as follows:

$$D = 0.9\ \lambda / \beta \cos\theta \quad (7)$$

where λ, β and θ are the X-ray wavelength, the full width at half maximum (FWHM) of the diffraction peak, and Braggs diffraction angle, respectively.

A JEOL 2300 model (Japan) was used to examine the surface morphology of the sample by scanning electron microscopy (SEM) and the percentage of constituent elements was evaluated by the energy dispersive X-rays analysis (EDAX) technique.

Sensitivity (S) is defined as the ratio of change in resistance of the sample on exposure to a test gas to the resistance in air [24, 25].

$$S = (Ra - Rg) / Ra = \Delta R / Ra \quad (8)$$

where *Rg* and *Ra* are the resistances of a sample in the presence and absence of a test gas, respectively, and ΔR the change in resistance. The sample was examined under different gases such as LPG, H_2, CO, CO_2, NH_3, O_2, Cl_2 and ethanol.

3. Results and Discussion

3.1. Structural Analysis by XRD

The X-ray diffraction pattern of the CTO thin film is shown in Fig. 2. It shows well defined broad diffraction peaks, indicating formation of polycrystalline phases. The diffraction peak indexing, done by matching with the Joint Committee on Powder Diffraction Standard (JCPDS) (no. 77-0452), clearly revealed formation of the SnO_2 phases with tetragonal structure. It was also seen that peaks corresponding to (110), (101), (200), (211) and (301) planes, with the (110) peak showing the highest intensity in all cases, implying that all the samples have a tetragonal crystal structure. No peaks belonging to Cr metal, Cr oxides or other impurity phases were detected within the sensitivity of our XRD measurements, indicating that the dopant was incorporated into the host lattice. These data indicate that Cr doping does not substantially alter the deposited crystal structure. The average crystallite size was determined using Scherrer equation which was observed to be 4 nm.

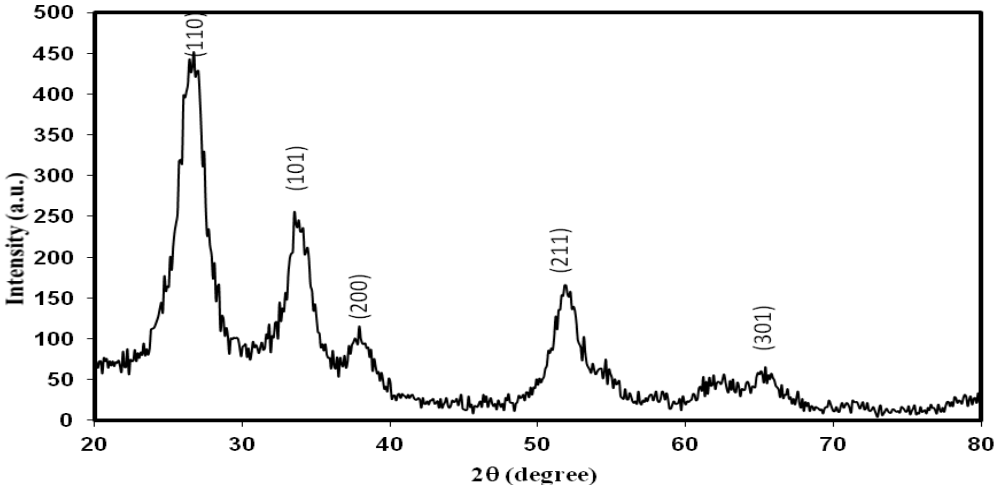

Fig. 2. X-ray diffraction pattern of CTO thin film.

3.2. Scanning Electron Microscopy (SEM) and Energy Dispersive X-rays Analysis (EDAX)

Fig. 3 shows SEM images of the CTO thin film on glass. It exhibit fractured surface morphology, covering the micropores on the surface. Chemical compositions of CTO thin film was investigated by energy dispersive X-ray analysis by X-ray spectroscopy (EDAX) as shown in Fig. 4. It indicates that thin film is composed of Sn, O and Cr, which is 29.82 at%, 60.75 at%, 9.43 at % respectively, demonstrating that the existence of chromium within the sample. It implies that actual atomic percentage ratio of Cr is less than the nominal composition (10 at%) in the solution. The difference between the actual and the nominal Cr concentration is probably due to the dilution of Cr ions in the SnO2 host matrix. It was found that the Cr doped SnO2 thin film was tin deficient and oxygen rich, indicating that the Cr doped SnnO2 thin film was non-stoichiometric.

3.3. Optical Properties

The optical energy band gap of CTO thin film was estimated from optical absorption measurement. The optical absorption spectrum for the CTO thin film is recorded in the wavelength range of 300–600 nm at room temperature shown in Fig. 5.

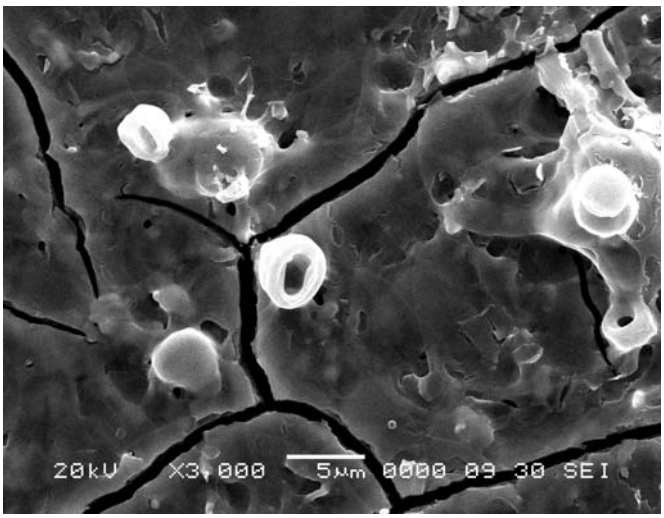

Fig. 3. SEM images of CTO thin film.

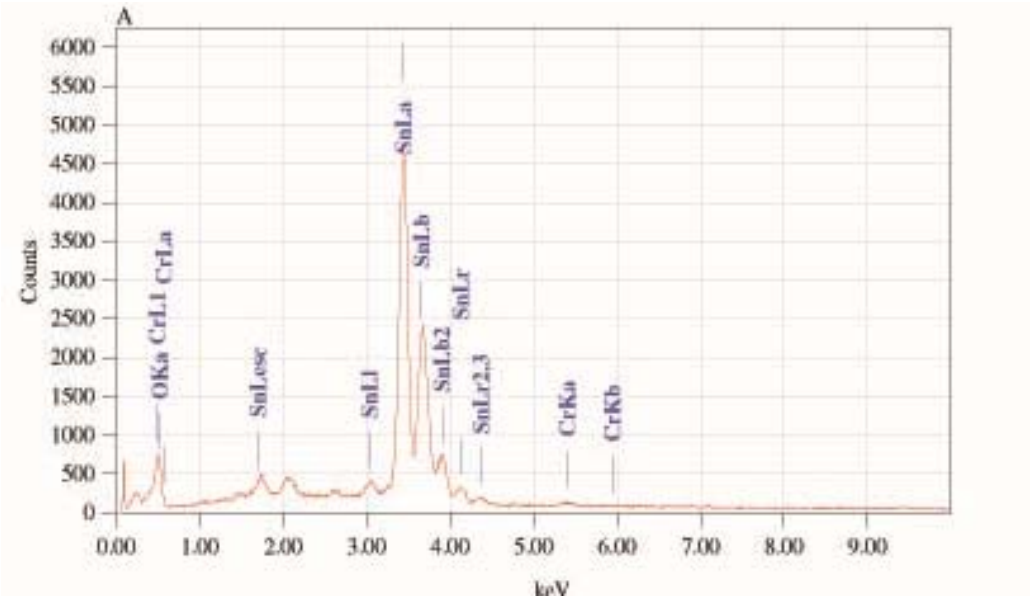

Fig. 4. EDAX spectra of CTO thin film.

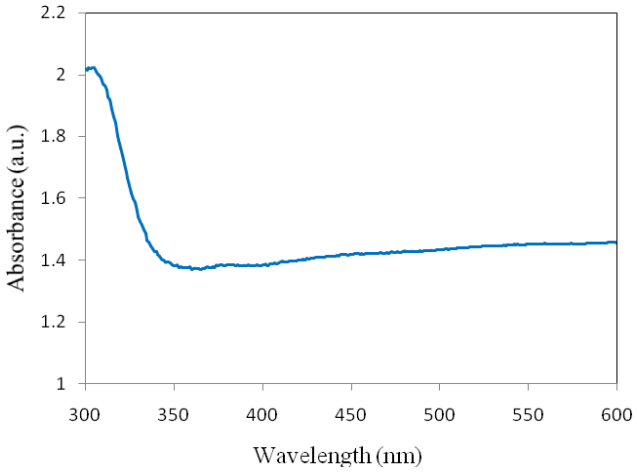

Fig. 5. UV-visible absorption spectra recorded for CTO thin film.

The optical absorption data were analyzed using the following classical relation of optical absorption in semiconductor near band edge [21]:

$$\alpha h\nu = A(h\nu - Eg)^n \tag{9}$$

where α is absorption coefficient, A is constant, Eg is the separation between bottom of the conduction band and top of the valence band, $h\nu$ the photon energy and n is a constant. The value of n depends on the probability of transition; it takes values as 1/2, 3/2, 2 and 3 for direct allowed, direct forbidden, indirect allowed and indirect forbidden transition respectively. Thus, if plot of $(\alpha h\nu)^2$ versus $(h\nu)$ is linear the transition is direct allowed. Extrapolation, of the straight-line portion to zero absorption coefficient ($\alpha = 0$), leads to estimation of band gap energy (Eg) values. Fig. 6 shows variation of $(\alpha h\nu)^2$ as a function of photon energy $(h\nu)$. The band gap energy, calculated from the spectrum for film is 3.54 eV.

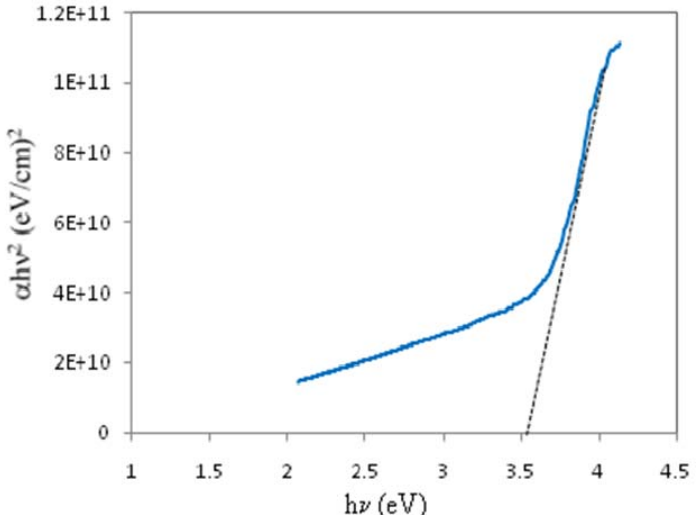

Fig. 6. Plot of the $(\alpha h\nu)^2$ vs. photon energy $(h\nu)$ for CTO thin film.

3.4. TEP Measurement

The thermoelectric power (TEP) was measured as a function of temperature in the range between 300 and 425 K. TEP is the ratio of thermally generated voltage to the temperature difference across the semiconductor. Diffusion of thermally generated majority charge carriers occurs from high temperature to the low temperature end, as a result of temperature difference (ΔT). This creates a positive space charge near high temperature end, which sets up an electric field or potential difference thereby giving rise to a thermal emf (ΔE). For SnO_2 material, conduction electrons originate from ionized defects such as oxygen vacancies, rendering n-type conductivity. The variation of the thermo emf with temperature difference (ΔT) for CTO thin film is shown in Fig. 7.

The rate of increment in TEP is higher in the range of ΔT from 355 to 375 K and thereafter slowed down. Initial increment is attributed to the increase in mobility of charge carriers and carrier concentration with rise in ΔT. The magnitude of TEP increases with rise in temperature difference (ΔT). The value of TEP lies in the range of 82–118 μVK^{-1}.

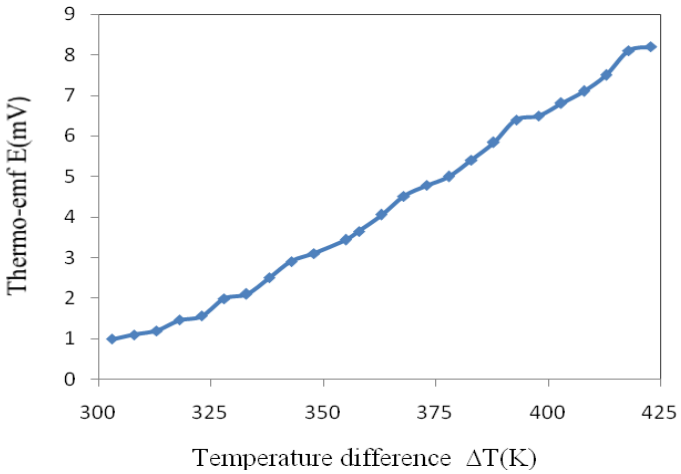

Fig. 7. Variation of the thermo emf with temperature difference (ΔT).

3.5. I-V Characteristics of CTO Thin Film

In this study Ag paint was used as the contacting electrode. The fermi levels in semiconductive CTO and metallic silver may not necessarily match and hence the possibility exists of forming Schotty barriers. *I-V* characteristics (see Fig. 8) were therefore measured at room temperature and the CTO films exhibited a linear dependence between current and voltage. This indicated an ohmic in nature of the silver contacts. Such linearity might arise due to essentially degenerately doped (high carrier concentration) SnO_2, where the tunneling barrier becomes small and a quasi-ohmic contact is observed [26].

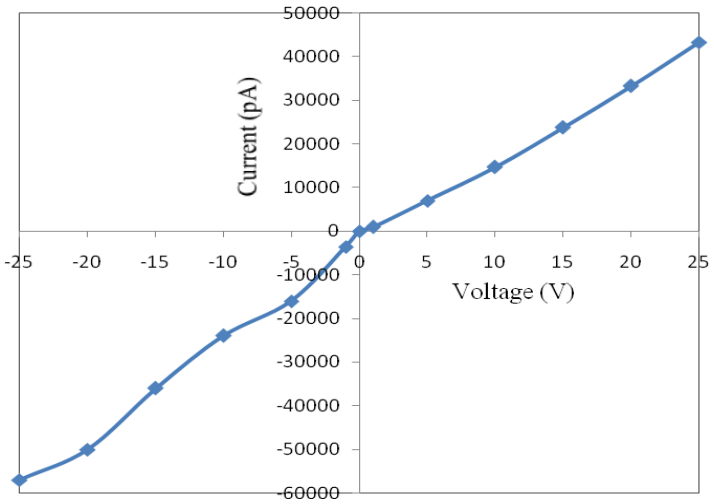

Fig. 8. I-V characteristics of CTO thin film.

3.6. Gas Sensing Properties

3.6.1. Principle of Ethanol Sensing Mechanism

The mechanism of the ethanol detection by CTO thin film can be described as follows: At first oxygen is adsorbed on the oxide layer when the sensitive film is heated at ambient at a temperature of 50 ^{o}C–550 ^{o}C. The adsorption of the oxygen forms ionic species such as O^{2-}, O_2^- and O^-. These oxygen

species when desorbed (desorption of O^2, O_2^- and O^- take place at 50 °C, 100 °C K and 550 °C, respectively), result in the increase or decrease of the conductance of thin film layer depending on the nature of gas. Its conductivity increases when the incoming gas is reducing type and decreases when it is oxidizing type. At the higher temperature range only O^- species will react with the contaminant gas. The reaction kinematics will proceed like this:

$$O_{2\,(gas)} \leftrightarrow O_{2\,(ads)} \tag{10}$$

$$O_{2\,(ads)} + e^- \leftrightarrow O_2^-{}_{(ads)} \tag{11}$$

$$O_{2\,(ads)} + e^- \leftrightarrow 2O^-_{(ads)} \tag{12}$$

The reaction between ethanol and ionic oxygen species takes place by two different ways:

$$C_2H_5OH_{\,(gas)} + O \leftrightarrow CH_3CHO + H_2O + e^- \tag{13}$$

$$C_2H_5OH_{\,(gas)} \leftrightarrow H + C_2H_5O_{\,(surface)} \tag{14}$$

$$C_2H_5OH \leftrightarrow H + CH_3CHO \tag{15}$$

$$CH_3CHO + O_{\,(bulk)} \leftrightarrow CH_3COOH + O_{\,(vacancies)} \tag{16}$$

3.6.2. Variation of Sensitivity to Ethanol with Operating Temperature

Fig. 9 shows the variation of sensitivity of CTO thin film sensor to 1000 ppm ethanol vapors with operating temperature. It is seen that for temperatures lower and higher than 300 °C, the sensitivity is less indicating 300 °C to be an optimum temperature. The highest sensitivity was obtained at 300 °C. It is reported that the highly active O^- is the dominant species in case of SnO_2 for temperature between 150 °C and 450 °C. The major adsorbed species in our films is therefore likely to be O^-. This adsorbed oxygen creates a space charge region near the film surface by extracting electrons from the material. Ethanol, being reducing in nature, removes adsorbed O^- species from the surface and re-injects the electrons back to the material, thereby reducing the resistance, which resulted in higher sensitivity.

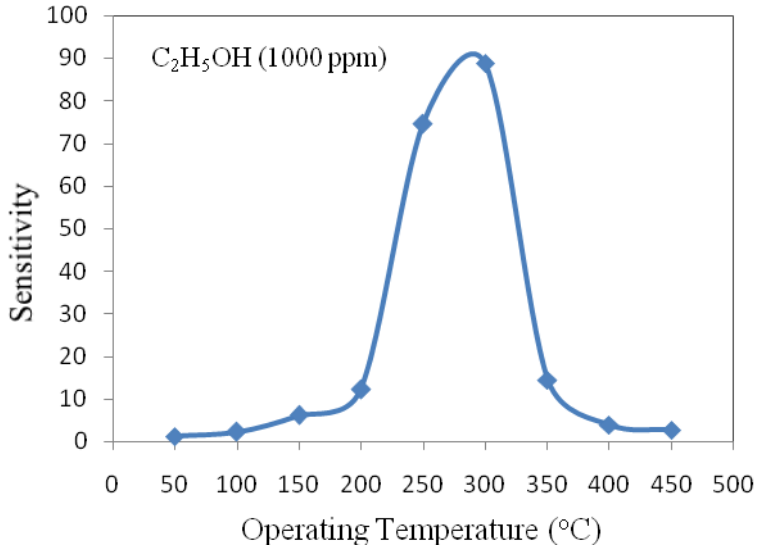

Fig. 9. Variation of sensitivity to ethanol with operating temperature.

3.6.3. Sensitivity with Ethanol Concentration

The dependence of the CTO thin film sensor's sensitivity on the concentrations of ethanol (10–1000 ppm) was investigated at 300 °C, and the result is shown in Fig. 10. As shown in the image, the CTO thin film sensors had good response to the ethanol even at low concentration of 10 ppm. Meanwhile, with increasing concentration of the ethanol, the sensitivity of the sensors sharply increased up to 1000 ppm. The rate increase of response was relatively larger up to 1000 ppm, smaller during 1000-1200 ppm and then saturates after 1000 ppm. Thus the active region of the sensor would be between 10-1000 ppm. At lower ethanol concentration, the monolayer of ethanol molecules would be expected to be formed on the surface which would interact with the surface more actively giving larger responses [27]. There would be multilayer of ethanol molecules on the sensor surface at the higher concentration resulting in saturation in sensitivity.

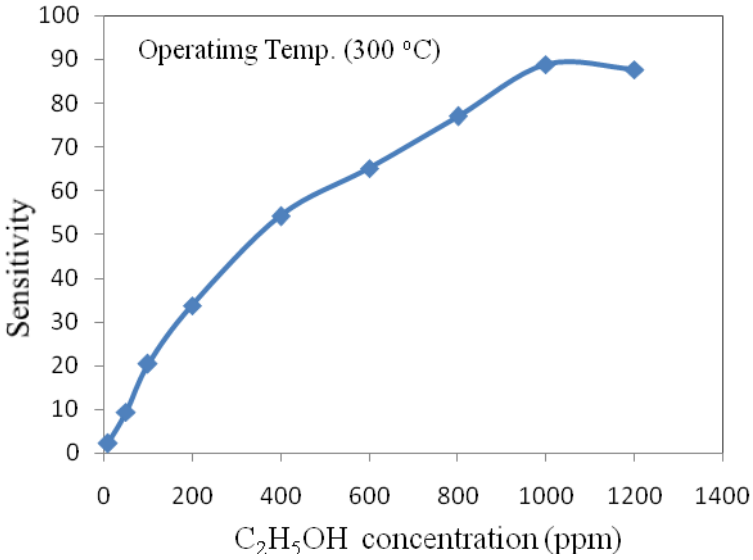

Fig. 10. Sensitivity with ethanol concentration at 300 °C.

3.6.4. Selectivity of Film against Different Gases

Besides ethanol, the sensing performances of the sensor to some other gases were also examined to depict its selectivity. Selectivity can be defined as the ability of a sensor to respond to a certain gas in the presence of different gases [21]. Fig. 11 depicts the selectivity of thin film sensor for ethanol (1000 ppm) at 300 °C. The film showed the high selectivity for ethanol among the following gases: LPG, NH_3, CO, CO_2, H_2, H_2S, O_2 and Cl_2.

3.6.5. Response Time and Recovery Time

The response time and recovery time (defined as the time required to reach 90 % of the final equilibrium value) are represented in Fig. 11. The response was quick (~8 s) while the recovery was fast (~36 s). The quick response may be due to faster oxidation of gas. The negligible quantity of the surface reaction product and its high volatility explains its quick response and fast recovery to its initial chemical status. Such a result indicates the good response speed of the sensors fabricated here.

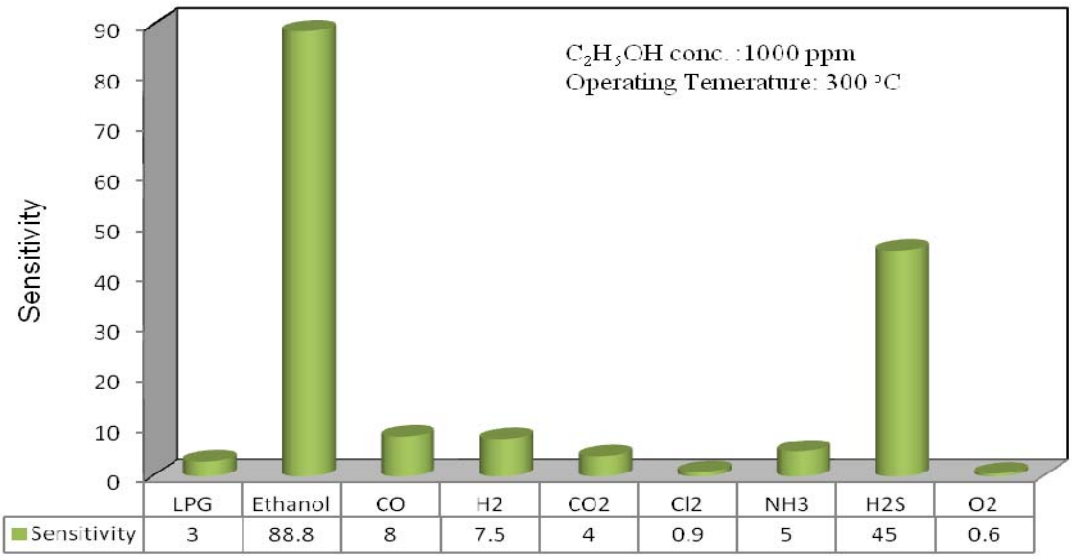

Fig. 11. Selectivity of film for various gases.

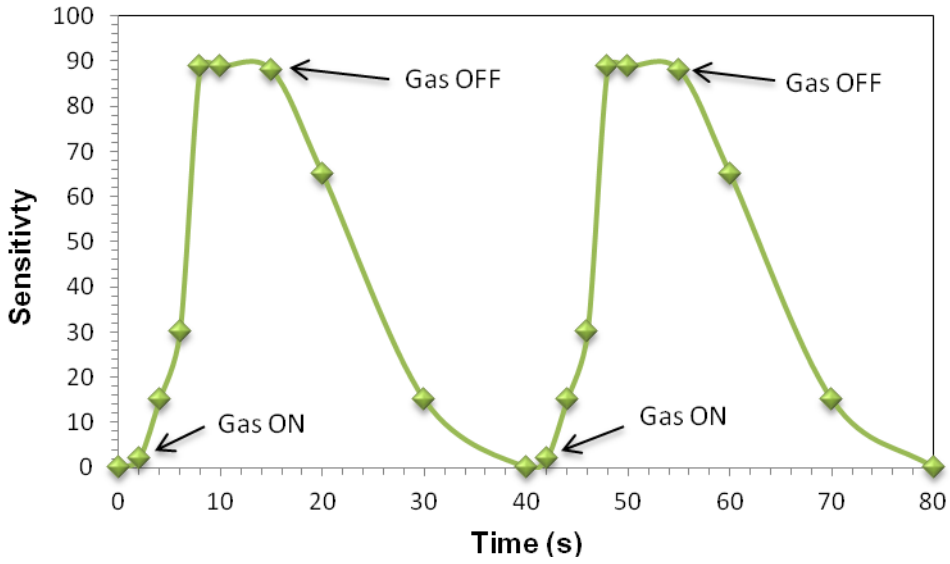

Fig. 11. Response and recovery time of CTO thin film sensor.

4. Conclusions

Based on the XRD, SEM, optical absorption, and gas sensing properties of CTO thin film prepared by spray pyrolysis technique (SPT) the following main points emerge:

1. Thin film showed the tetragonal structure with a strong (110) preferred orientation. Cr incorporation did not significantly change the crystal structure of SnO_2. The average crystallite size was 4 nm.
2. Scanning electron micrograph shows the micropores on the surface of thin film.
3. Band gap obtained from UV- spectra is 3.54 eV.
4. CTO thin film was observed to be more sensitive to ethanol than the responses to other gases. The sensor has good selectivity to ethanol against LPG, CO_2, NH_3, C_2H_5OH and Cl_2. The sensor showed quick response (8 s) and fast recovery (36 s).
5. The results demonstrate that CTO thin films have excellent potential applications for fabrication high performance ethanol sensors.

Acknowledgements

The authors are thankful to University Grants Commission, DST, New Delhi and BCUD, University of Pune, Pune for providing financial support. Thanks to The Principal, Arts, Commerce and Science College, Nandgaon for providing laboratory facilities for this work.

References

[1]. G. Korotcenkov, I. Boris, V. Brinzari, Yu. Luchkovsky, G. Karkotsky, V. Golovanov, A. Cornet, E. Rossinyol, J. Rodriguez, A. Cirera, Gas sensing characteristics of one-electrode gas sensors on the base of doped In_2O_3 ceramics, *Sensors and Actuators B*, Vol. 103, 1-2, 2004, pp. 13-22.

[2]. N. Barsan and U. Weimar, Understanding the Fundamental Principles of Metal Oxide Based Gas Sensors: the Example of CO Sensing with SnO_2 Sensors in the Presence of Humidity, *Journal of Physics: Condensed Matter*, Vol. 15, 2003, pp. R1–R27.

[3]. N. Yamazoe, New approaches for improving semiconductor gas sensors, *Sensors and Actuators B*, Vol. 5, 1991, pp. 7–19.

[4]. U. Kirner, K. D. Schierbaum, W. Göpel, B. Leibold, N. Nicoloso, W. Weppner, D. Fischer and W. F. Chu., Low and high temperature TiO_2 oxygen sensors, *Sensors and Actuators B*, Vol. 1, 1990, pp. 103–107.

[5]. G. N. Advani and L. Nanis, Effects of humidity on hydrogen sulfide detection by SnO_2 solid state gas sensors, *Sensors and Actuators*, Vol. 2, 1981/1982, pp. 201-206.

[6]. T. W. Capehart and S. C. Chang, The interaction of tin oxide films with O_2, H_2, NO, and H_2S, *The Journal of Vacuum Science and Technology*, Vol. 18, 1981, pp. 393–397.

[7]. Y. Liu, E. Koep and M. Liu, A Highly Sensitive and Fast-Responding SnO_2 Sensor Fabricated by Combustion Chemical Vapor Deposition, *Chemical Material*, Vol. 17, 15, 2005, pp. 3997–4000.

[8]. S. Phadungdhitidhada, S. Thanasanvorakun, P. Mangkorntong, S. Choopun, N. Mangkorntong, D. Wongratanaphisan, SnO_2 nanowires mixed nanodendrites for high ethanol sensor response, *Current Applied Physics*, Vol. 11, 6, 2011, pp. 1368-1373.

[9]. H. Li, J. Xu, Y. Zhu, X. Chen and Q. Xiang, Enhanced gas sensing by assembling Pd nanoparticles onto the surface of SnO_2 nanowires, *Talanta*, Vol. 82, 2010, pp. 458–463.

[10]. I. S. Hwang, J. K. Choi, S. J. Kim, K. Y. Dong, J. H. Kwon, B. K. Ju, J. H. Lee, Enhanced H_2S sensing characteristics of SnO_2 nanowires functionalized with CuO, *Sens. Actuators B,* Vol. 142, 2009, pp. 105–110.

[11]. N. V. Hieu, Highly reproducible synthesis of very large-scale tin oxide nanowires used for screen-printed gas sensor, *Sens. Actuators B*., Vol. 144, 2010, pp. 425–431.

[12]. J. Zhang, S. Wang, Y. Wang, M. Xu, H. Xia, S. Zhang, W. Huang, X. Guo and S. Wu, Facile synthesis of highly ethanol-sensitive SnO_2 nanoparticles, *Sens. Actuators B*., Vol. 139, 2009, pp. 369–374.

[13]. L. Xi, D. Qian, X. Tang and C. Chen, High surface area SnO_2 nanoparticles: synthesis and gas sensing properties, *Mater. Chem. Phys.,* Vol. 108, 2008, pp. 232–236.

[14]. D. Kohl, Surface processes in the detection of reducing gases with SnO_2-based devices, *Sensors and Actuators,* Vol. 18, Issue 1, 1989, pp. 71-113.

[15]. H. Ogawa, M. Nishikawa, and A. Abe, Hall measurement studies and an electrical conduction model of tin oxide ultrafine particle films, *J. App. Phys*., Vol. 53, 1982, pp. 4448-4455.

[16]. D. Kohl, Function and applications of gas sensors, *Journal of Physics D: Applied Physics*, Vol. 34, 2001, p. R125.

[17]. C. N. R. Rao, A. R. Raju, and K. Vijayamohanan, New Materials, *Narosa Publishing House*, New Delhi, India, 1992, pp. 1.

[18]. K. Fukui and S. Nishida, CO gas sensor based on Au-La_2O_3 added SnO_2 ceramics with siliceous zeolite coat. Sensor, *Sens. Actuators B*, Vol. 45, 1997, pp. 101-106.

[19]. Hae Won Cheong, Hee Sook Park Kim, Ki Hyun Yoon, Role of Additives in Tin Oxide-Based Sensors for Alcohols, *Key Engineering Materials*, Vol. 277 – 279, 2005, pp. 403-409.

[20]. P. S. Patil, Versatility of spray pyrolysis technique, *Material Chemistry and Physics*, Vol. 59, 1999, pp. 185-198.

[21]. Ganesh E. Patil, D. D. Kajale, P. T. Ahire, D. N. Chavan, N. K. Pawar, S. D. Shinde, V. B. Gaikwad and G. H. Jain, Synthesis, characterization and gas sensing performance of SnO_2 thin films prepared by spray pyrolysis, *Bulletin of Material Science*, Vol. 34, No. 1, February 2011, pp. 1–9.

[22]. Ganesh E. Patil, D. D. Kajale, D. N. Chavan, N. K. Pawar, V. B. Gaikwad, G. H. Jain, Spray pyrolyzed polycrystalline tin oxide thin film as hydrogen sensor, *Sensors & Transducers*, Vol. 120, Issue 9, September 2010, pp. 70-79.
[23]. B. D. Cullity, Elements of X-ray diffraction, *Addison-Wesley Publishing Co.,* USA, 1956.
[24]. G. H. Jain, S. B. Nahire, Ganesh E. Patil, D. D. Kajale, S. D. Shinde, D. N. Chavan and V. B. Gaikwad, Cr_2O_3-doped $BaTiO_3$ as an Ammonia Gas Sensor, *New Developments and Applications in Sensing Technology, Lecture Notes in Electrical Engineering*, Vol. 83, 2011, pp. 157-167.
[25]. S. D. Shinde, G. E. Patil, D. D. Kajale, V. B. Gaikwad and G. H. Jain, Gas sensing performance of nanostructured ZnO thick film resistors, *International Journal of Nanoparticles*, (Article in press).
[26]. S. M. Sze, Semiconductor Devices, Physics and Technology, *Wiley*, New York, 1985, pp. 169.
[27]. Hae-Won Cheong and Man-Jong Lee, Sensing characteristics and surface reaction mechanism of alcohol sensors based on doped SnO_2, *Journal of Ceramic Processing Research*, Vol. 7, No. 3, 2006, pp. 183-191.

2012 Copyright ©, International Frequency Sensor Association (IFSA). All rights reserved.
(http://www.sensorsportal.com)